PHOTOMASK

BACUS—The international technical group of SPIE dedicated to the advancement of photomask technology.

PUV20 - Zeiss Winner 1st Place Student Poster

Alkyltin Keggin clusters as EUVL photoresist technology

Rebecca D. Stern, Department of Materials Science and Engineering, University of California Berkeley, Berkeley, CA, 94720

Danielle C. Hutchison, May Nyman, and Morgan R. Olsen, Department of Chemistry, Oregon State University, Corvallis, OR, 97331, USA

Lev N. Zakharov, Department of Chemistry and Biochemistry, University of Oregon, Eugene, OR, 97403, USA

Kristin A. Persson, Department of Materials Science and Engineering, University of California Berkeley, Berkeley, CA, 94720, USA; Lawrence Berkeley National Laboratory, Berkeley, CA, 94720, USA

ABSTRACT

Extreme ultraviolet lithography is the newest technique to keep up with Moore's law and create smaller integrated circuit feature sizes. However, novel photoresist materials must be used in order to withstand the high energy beam (λ=13.5nm). Metal-oxo clusters have been proposed as one photoresist solution, and specifically the most promising is a sodium-centered tin-Keggin cluster. A simple one-step synthesis was developed to produce a Na-Sn Keggin cluster, without the need for heating, filtration, or recrystallization. However, the product was a mixture of the β-isomer (β-$NaSn_{12}$) and the γ-isomer (γ-$NaSn_{12}$), which share the formula $[(MeSn)_{12}(NaO_4)(OCH_3)_{12}(O)_4(OH)_8]^{1+}$. For fundamental studies on the lithographic mechanisms occurring during exposure to be successful, a pure and stable isomer is desired. Computational modeling was recruited to determine the ground state energy of all five uncapped isomers in this Na-Sn Keggin system. Additionally, the inclusion of one or two tin atoms to the uncapped structure, called capping, altered which isomers were stabilized. Computations were also employed to evaluate the influence of this capping strategy for the single-capped β-isomer (β-$NaSn_{13}$), the single-capped α-isomer (α-$NaSn_{13}$), the single-capped γ-isomer (γ-$NaSn_{13}$), and the double-capped γ-isomer (γ-$NaSn_{14}$). Density functional theory (DFT) was used to obtain the hydrolysis Gibbs free energy and HOMO-LUMO gap, which led to the stability ranking: β-$NaSn_{12}$ > γ-$NaSn_{12}$ > α-$NaSn_{12}$ > δ-$NaSn_{12}$ > ε-$NaSn_{12}$ for uncapped clusters, which was consistent which experimental observations. The uncapped isomers were computationally evaluated to be more stable than their respective single-capped analogues. However, the double-capped γ-$NaSn_{14}$ was more stable than either the uncapped or single-capped clusters. Therefore, capping has shown to be a useful tool in exploring the stability landscape of these Keggin clusters to promote a pure and stable material for the next generation EUV lithography photoresists. And noteworthy, this sodium-centered tin-Keggin ion represents the only Keggin ion family so far, that favors the isomers of lower symmetry.

1. Introduction

With integrated circuit manufacturers aiming to produce sub-10nm feature sizes, extreme ultraviolet lithography (EUVL) is perceived as the next developing technology, at a wavelength of only 13.5nm.[1] The challenges with using polymer-based photoresists for EUVL can be eliminated by using metal-oxo cluster photoresists. Metal-oxo clusters are smaller than the bulky carbon chains in the polymer-based resists, thus preventing pattern collapse. Also, metal-oxo clusters are more durable during the lithographic etching step. Metal-oxo systems previously investigated as potential photoresist materials include hafnium, antimony, and

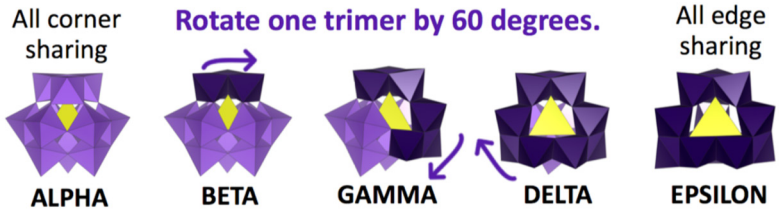

Figure 1. Trimer rotation to obtain five Keggin isomers α, β, γ, δ, and ε.

BACUS NEWS

MARCH 2020
VOLUME 36, ISSUE 3

SPIE.

11147-72

EDITORIAL

Mask Blank Diversity

Thomas Scherübl, Carl Zeiss SMT GmbH

When I started to work for the photomask industry about 15 years ago, I was puzzled about the meaning of "BACUS". I learned that "BACUS" stands for "Bay Area Chromium Users". This comes from a time (I think the 80s or so) when the semiconductor industry was predominately located in the Bay Area and photomasks used chromium as the one and only absorber material. Chromium has been doing its job as an absorber for quite a time as it has the properties needed for an absorber material: block light and somehow easy to pattern and clean.

As Moore's Law progressed, features on the mask and the wavelengths of the scanner became smaller. Better contrast for imaging was required which resulted e.g. in the introduction phase shifting masks based on a MoSi blank material. Still, the number of blank types was quite limited at that time. With the extension of 193nm immersion lithography additional parameters like mask durability during exposure or cleaning began to play a role. These trends boosted the number of so-called new mask materials which were introduced for 193nm immersion lithography.

Currently, EUV is entering high volume manufacturing and the same trend already begins to start for EUV blanks. For a long time, it seemed that EUV will use only two absorber types. However, mask 3D effects which are limiting the imaging performance are driving research for new thinner absorber materials and phase shifting masks. This was the topic of several talks at the last BACUS/EUVL conference (see also Bacus News, October 2019, Vol. 35, Issue 10). For new absorbers, a variety of new candidate materials exist. These materials need to provide not only good imaging performance but need to be manufacturable, too. For the selection of proper materials, it is crucial to investigate and optimize the processes with regards to low defect count, etch and clean performance, as well as repairability.

Introducing new blank materials will require the corresponding adjustments to the infrastructure in mask manufacturing. For EUV masks and the tolerances involved, these changes tend to be more complex than in earlier times. For achieving this in time for high volume production, close cooperation in the mask industry is more important than ever. There it is beneficial for the whole industry to align efforts already in an early stage among blank vendors, mask manufacturers, and tool suppliers for etching, cleaning, and repair.

BACUS

N • E • W • S

BACUS News is published monthly by SPIE for *BACUS*, the international technical group of SPIE dedicated to the advancement of photomask technology.

Managing Editor/Graphics Linda DeLano
SPIE Sales Representative, Exhibitions, and Sponsorships Melissa Valum
BACUS Technical Group Manager Marilyn Gorsuch

SPIE.

P.O. Box 10, Bellingham, WA 98227-0010 USA
Tel: +1 360 676 3290
Fax: +1 360 647 1445
SPIE.org
help@spie.org

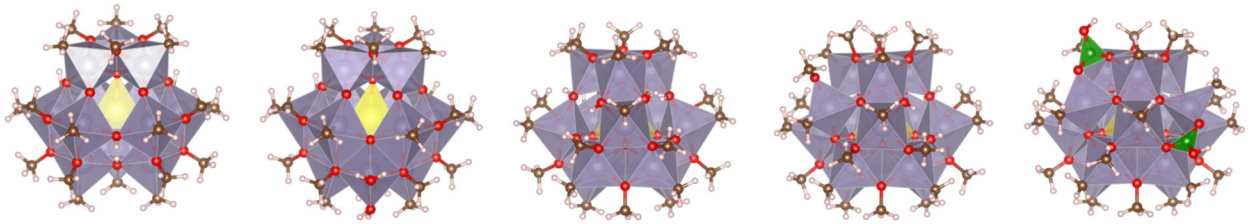

Figure 2. (a) uncapped β-$NaSn_{12}$, (b) single-capped β-$NaSn_{13}$, (c) uncapped γ-$NaSn_{12}$, (d) single-capped γ-$NaSn_{13}$, (e) double-capped γ-$NaSn_{14}$. Tin are purple octahedra, sodium is central yellow tetrahedra, carbon are brown, hydrogen are white, and boron are green.

tin clusters.[2–6] These systems have a high EUV atomic absorption cross-section, needed for proper resist functionality.[7] Each system had their limitations however. Hafnium-based clusters demonstrated 8nm resolution but resulted in background condensation.[2] Antimony-oxo clusters had EUV sensitivity but pattern collapse limited high resolution.[3] The tin-oxo "football" cluster prevented background condensation, but the synthesis was difficult.[4] A capped sodium-centered organotin-oxo Keggin cluster produced high aspect ratio and dense line patterns with helium ion beam lithography, but synthesis of the structure was difficult leading to poor reproducibility and low yields.[5,6] It is thought that the cleavage of the Sn-C bond of the terminal butyl ligands in this material is the cause of the change in the solubility of this photoresist.[8] In order to evaluate this system in more depth, a simplified synthesis strategy was required to further investigate the possibilities of a sodium center organotin-oxo Keggin cluster as a photoresist for EUV lithography.

Hutchison and coworkers recently discovered a simple one-step synthesis for the Na-Sn Keggin system that proceeds at room temperature and does not require any filtration or recrystallization.[9] This synthesis strategy successfully made the $[(MeSn)_{12}(NaO_4)(OCH_3)_{12}(O)_4(OH)_8]^{1+}$, which is an uncapped Keggin cluster denoted β-$NaSn_{12}$. However, this synthesis led to a mixture of uncapped β-$NaSn_{12}$ and uncapped γ-$NaSn_{12}$ isomers. Computational studies were recruited to investigate this dilemma and unknown cause. Since the Keggin geometry has 5 possible isomers, all 5 uncapped $NaSn_{12}$ isomers α, β, γ, δ, and ε, were computationally modeled in this paper. To evaluate the influence of capping on the prevention of isomerization between uncapped β-$NaSn_{12}$ and uncapped γ-$NaSn_{12}$, the experimentally observed capped β-$NaSn_{13}$ and γ-$NaSn_{13}$, as well as the most recently synthesized double capped γ-$NaSn_{14}$ were computationally modeled in this paper as well.[9,10] The advantages of using computational modeling tools is to be able to evaluate the thermodynamic stability of experimental as well as theoretical isomers of a given system. The calculated thermodynamic landscape of the isomers enables comparison of the isomer stability and hence interpretation of experimental results. Ideally, computational results will guide synthesis design, being able to determine the influential factors that drive stability between isomers and predict new structures.

2. Description of Structures

2.1 The Keggin geometry

The Keggin cluster was first structurally characterized in 1934 by J.F. Keggin.[11] It contains a heteroatom metal center in a 4-coordinate environment. Surrounding this are four trimer units. Each trimer unit consists of three metals in a 6-coordinate environment. The three octahedra are edge-sharing within the trimer unit. The α-isomer is defined as having its four trimer units connected by corner-sharing between trimers, resulting in T_d symmetry, as shown in Figure 1. If one trimer unit is rotated by 60 degrees, the β-isomer is obtained which still exhibits only corner-sharing trimers but with a reduced symmetry of C_{3v}. Continuing this process of successive trimer rotations of 60 degrees, the γ-isomer of C_{2v} symmetry is obtained. Finally, a rotation of a third trimer yields the δ-isomer and a fourth trimer rotation yields the ε-isomer, possessing C_{3v} and T_d symmetries, respectively.

2.2 Situation I: Mixed β/γ-$NaSn_{12}$

The one-step synthesis strategy developed by Hutchison *et al*. occurred at room temperature and did not require any filtration or recrystallization.[9] However, ^{119}Sn-NMR and single-crystal x-ray diffraction showed a mixture of β-$NaSn_{12}$ and γ-$NaSn_{12}$. To investigate the isomerization, all five uncapped Na-Sn Keggin isomers (α, β, γ, δ, ε) were computationally modeled. They all were given the same formula: $[(MeSn)_{12}(NaO_4)(OCH_3)_{12}(O)_4(OH)_8]^{1+}$. The β-$NaSn_{12}$ and γ-$NaSn_{12}$ clusters are shown in Figure 2a and 2b, respectively. To decrease the computational cost and complexity of these models, the butyl Sn-terminal ligands were replaced with methyl ligands, a common practice.[12] In this Na-Sn Keggin system, the central heteroatom is sodium. Each trimer unit of the Keggin is comprised of three $MeSnO_5$ octahedra with a methyl terminal ligand on each tin atom. The three bridging oxygens within each trimer unit (12 total O^{2-}) are methoxy ligands. The bridging oxygens between the four trimer units (12 total O^{2-}) are oxo or hydroxyl ligands. The overall charge of the structures is determined by the total number of hydroxyl ligands. The location of the hydroxyl ligands impacts the hydrolysis Gibbs free energy and care was taken to obtain the lowest energy conformation. Although the hydrogen location cannot be inferred from the x-ray diffraction data, mass spectrometry identified the overall charge of the structures and bond-valence sum helped guide the hydroxyl ligand placement.

2.3 Situation II: Single-capped β-$NaSn_{13}$

Saha *et al*. in 2017 produced a single-capped β-$NaSn_{13}$.[5] However, authors found impurities of uncapped $NaSn_{12}$ isomers and Sn_{12} (i.e. the 'football' cluster $[(RSn)_{12}O_{14}(OH)_6]^{2+}$, R=alkyl) co-crystallized with β-$NaSn_{13}$ in unknown quantities, as determined with electrospray ionization mass spectroscopy (ESI-MS) and ^{119}Sn-NMR. The computationally modeled β-$NaSn_{13}$ was assigned a formula of $[(MeSn)_{12}(NaO_4)(OCH_3)_{12}(O)_8(OH)_4(Sn(H_2O)_2)]^{1+}$ which is exactly consistent with the experimental crystal structure determined by ESI-MS.[9] The cap position and bonding for theoretical α-$NaSn_{13}$ was modeled after β-$NaSn_{13}$ since these two isomers exhibit similar symmetries and capping "windows" as compared to γ-$NaSn_{13}$. The cap on β-$NaSn_{13}$ and α-$NaSn_{13}$ is a 6-coordinate tin, with four bonds to the cluster in the tetragonal window. The two terminal ligands are waters. The single-capped β-$NaSn_{13}$ is shown in Figure 2c.

2.4 Situation III: Single-capped γ-$NaSn_{13}$

A different synthesis strategy conducted by Hutchison *et al.* produced single-capped γ-$NaSn_{13}$.[9] However, crystals of both γ-$NaSn_{13}$ and uncapped β-$NaSn_{12}$ were isolated from the same closed vial.[9] This computational study modeled the γ-$NaSn_{13}$ as $[(MeSn)_{12}(NaO_4)(OCH_3)_{12}(O)_6(OH)_6(Sn(Me)(OCH_3))]^{1+}$ as shown in Figure 2d. The cap is a 5-coordinate tin, with three bonds to the cluster in one of the pentagonal windows adjacent to the edge sharing trimer units. The two terminal ligands are methyl and methoxy.

2.5 Situation IV: Double-capped γ-$NaSn_{14}$

Zhu *et al.* very recently synthesized the double-capped γ-$NaSn_{14}$ in 2019.[10] This synthesis strategy successfully prevented isomerization, yielding pure γ-$NaSn_{14}$. Two 5-coordinate tin caps are found on the structure, one in each pentagonal window on either side of the edge shared between two trimer units. The terminal ligands are a butyl chain (modeled as methyl) and an oxygen atom from a $BO_2(OH)$ ligand. The two borate ligands provide a bridge between the tin cap and they each replace one methoxy ligand within a trimer unit. The authors believe the borate group stabilizes the cap, which in turn stabilizes the Keggin cluster. This structure is shown in Figure 2e.

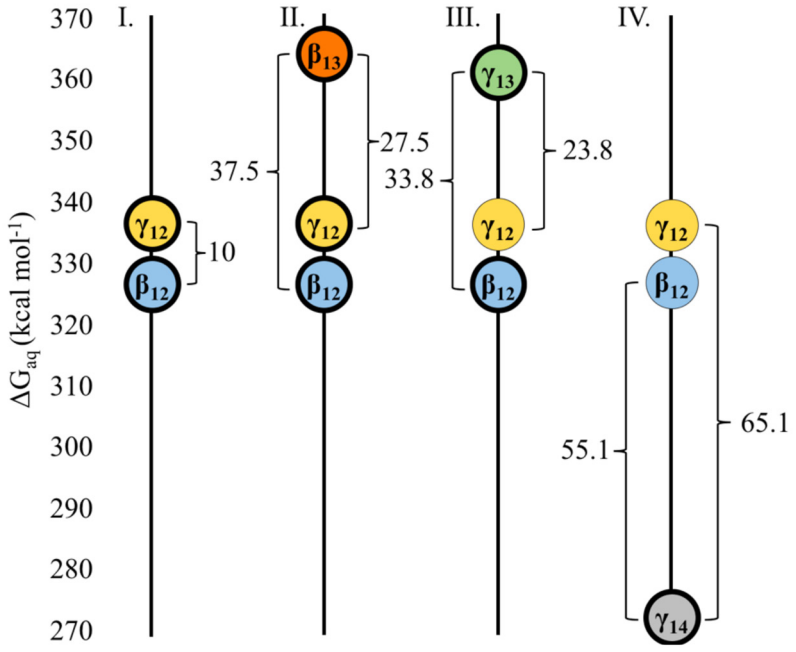

Figure 3. Four synthesis strategies (I, II, III, IV) and their experimentally observed results (bold-circled isomers). Hydrolysis Gibbs free energies of all relevant isomers are included. Blue = β-$NaSn_{12}$, Yellow = γ-$NaSn_{12}$, Red = β-$NaSn_{13}$, Green = γ-$NaSn_{13}$, Gray = γ-$NaSn_{14}$.

3. Methodology

3.1 Approach

The experimentally isolated clusters were computationally modeled. These consisted of the two uncapped isomers (β-$NaSn_{12}$, γ-$NaSn_{12}$), the two single-capped isomers (β-$NaSn_{13}$, γ-$NaSn_{13}$), and the one double-capped isomer (γ-$NaSn_{14}$). Additionally, theoretical clusters (which have never been experimentally isolated) of the Na-Sn system were also modeled. These included three uncapped isomers (α-$NaSn_{12}$, δ-$NaSn_{12}$, ε-$NaSn_{12}$), and one single-capped isomer (α-$NaSn_{13}$), bringing the total number of systems investigated to nine.

We determined the hydrolysis Gibbs free energy (ΔG_{aq}) in solution by using a thermodynamic cycle in which the hydrolysis energy is the sum of the corresponding gas-phase Gibbs free energy (ΔG_{gas}) and the Gibbs free energies of solvation ΔG_{solv} as seen in Equation 1. The thermodynamic cycle is used to reduce errors when calculating the solvation energy and comparing structures of different formula.[13–16] The gas-phase Gibbs free energy contains a correction term that takes into account the enthalpy, entropy, and temperature of the system when a frequency analysis is conducted. The term "n" is the coefficient of that species. An example of this thermodynamic cycle using β-$NaSn_{12}$ is shown in Scheme 1. The dielectric constant for the solvent model was set to ~78.36, consistent with water.

$$\Delta G_{aq} = \Delta G_{gas} + \sum_{i=1}^{Nproducts} n_i \Delta G_i^{solv} - \sum_{j=1}^{Nreactants} n_j \Delta G_j^{solv} \quad (1)$$

3.2 Computational details

The geometry of each cluster was first optimized using Gaussian 09 in the gas phase using the B3LYP functional.[17] The basis set 6-31G(d) was used for elements Na, Ca, C, H, and O, while the basis set LANL2DZ was used for the element Sn.[18,19] A subsequent frequency calculation was performed to verify the absence of imaginary vibration modes to confirm that the system is in a stable/metastable state. An effective core potential LANL2DZ was used for Sn. The geometry was further optimized in water using the continuum solvation model SMD.[20] The electronic energy was refined using a B3LYP single point with the basis set 6-311+G(d,p) for elements Na, Ca, C, H, and O, and basis set LANL2DZ for Sn.[21] The solvation energy was computed using a B3LYP/6-31G(d) single point with SMD for water (ε=78.36).

4. Results and Discussion

The hydrolysis Gibbs free energy in kcal mol^{-1} and HOMO-LUMO gap in eV are listed in Table 1 for each of the nine clusters investigated. The more stable clusters should exhibit a relatively low hydrolysis Gibbs free energy and a relatively large HOMO-LUMO gap. In our case, the stability ordering is evaluated by the hydrolysis Gibbs free energy. The HOMOLUMO gaps are too close in energy to conclusively determine the isomer stability ordering, but rather used to support the results from the Gibbs free energy.

The uniqueness of the tin-oxo Keggin system is that it prefers the less symmetric isomers, β and γ. To our knowledge, no other Keggin cluster systems have been discovered where the β and γ isomers are the most

Scheme 2. Thermodynamic cycle for β-$NaSn_{12}$.

$$12\,Sn(H_2O)_6^{4+}{}_{(aq)} + 6\,Na(H_2O)_6^{+}{}_{(aq)} + 3\,CO_{2(aq)} + 21\,CH_{4(aq)} \xrightarrow{\Delta G_{aq}} 48\,H_3O^+_{(aq)} + 8\,H_2O_{(aq)} + C_{24}H_{80}NaO_{28}Sn_{12}^{+}{}_{(aq)}$$

$$\downarrow -\Delta G^{solv}_{Sn(H_2O)_6^{4+}} \quad \downarrow -\Delta G^{solv}_{Na(H_2O)_6^{+}} \quad \downarrow -\Delta G^{solv}_{CO_2} \quad \downarrow -\Delta G^{solv}_{CH_4} \qquad \uparrow \Delta G^{solv}_{H_3O^+} \quad \uparrow \Delta G^{solv}_{H_2O} \quad \uparrow \Delta G^{solv}_{C_{24}H_{80}NaO_{28}Sn_{12}^{+}}$$

$$12\,Sn(H_2O)_6^{4+}{}_{(g)} + 6\,Na(H_2O)_6^{+}{}_{(g)} + 3\,CO_{2(g)} + 21\,CH_{4(g)} \xrightarrow{\Delta G_{gas}} 48\,H_3O^+_{(g)} + 8\,H_2O_{(g)} + C_{24}H_{80}NaO_{28}Sn_{12}^{+}{}_{(g)}$$

Table 1. Hydrolysis Gibbs free energy (kcal mol^{-1}) and HOMO-LUMO gap (eV) of uncapped and capped Na-Sn clusters.

Cluster	Hydrolysis Gibbs Free Energy (kcal mol^{-1})	HOMO-LUMO gap (eV)
ε-$NaSn_{12}^{1+}$	386.6	5.87
α-$NaSn_{13}^{1+}$	369.7	5.17
β-$NaSn_{13}^{1+}$	364.9	5.28
γ-$NaSn_{13}^{1+}$	361.2	5.80
δ-$NaSn_{12}^{1+}$	347.3	6.09
α-$NaSn_{12}^{1+}$	342.7	6.20
γ-$NaSn_{12}^{1+}$	337.4	5.91
β-$NaSn_{12}^{1+}$	327.4	6.24
γ-$NaSn_{14}$	272.3	6.04

stable. Traditional polyoxometalates like the W- and Mo-Keggin clusters prefer the α and β isomers.[22] The Al-Keggin and Sb-Keggin favor the ε isomer.[12,23] And the Cr-Keggin has been recently synthesized as the δ-isomer.[24,25] A visual guide for the joint results of the four synthesis strategies (bolded values) and the relevant isomer energy differences are shown in Figure 3. The hydrolysis Gibbs free energy differences between the uncapped clusters are similar in magnitude to previously reported polyoxometalates.[26,27] Synthesis strategy I produced a mixture of uncapped β-$NaSn_{12}$ and γ-$NaSn_{12}$ clusters, as shown in Figure 3.9 The calculated relative instability of the uncapped α-$NaSn_{12}$ compared to the uncapped β-$NaSn_{12}$ and γ-$NaSn_{12}$ is in accordance with our experimental results, such that it has not been experimentally observed.[9] We hypothesize that the reason γ-$NaSn_{12}$ is 10 kcal mol^{-1} more unstable than β-$NaSn_{12}$ is due to the electrostatic repulsion from the Sn-Sn edge-sharing distance being 3.26 Å, while the Sn-Sn corner-sharing distance is ~3.4-3.5 Å.[9]

Synthesis strategy II performed by Saha *et al.* in 2017 produced a charge neutral single-capped β-$NaSn_{13}$.[5] However, authors found impurities of uncapped $NaSn_{12}$ and Sn_{12} (i.e. the 'football' cluster $[(RSn)_{12}O_{14}(OH)_6]^{2+}$, R=alkyl) cocrystallized with β-$NaSn_{13}$ in unknown quantities, as determined with ESI-MS and ^{119}Sn-NMR. Results for this situation are shown in Figure 3. The computational results performed in this study indicate that single-capped β-$NaSn_{13}$ is more unstable than uncapped β-$NaSn_{12}$ by 37.5 kcal mol^{-1} and uncapped γ-$NaSn_{12}$ by 27.5 kcal mol^{-1}. One interpretation of these results is that a hydrolysis Gibbs free energy difference of 37.5 kcal mol^{-1} between a capped and uncapped system is not sufficient to prevent the respective uncapped system from forming. We also note that it is possible that specific isomers explicitly interact more strongly with the solution, which would not be captured in our mean-field solvation approach.

Synthesis strategy III produced single-capped γ-$NaSn_{13}$ with the presence of uncapped β-$NaSn_{12}$.[9] This result is indicated in Figure 3; the isomers that are circled in bold are the isomers that were observed with this synthesis strategy. The computational results indicate that single-capped γ-$NaSn_{13}$ is more unstable than uncapped β-$NaSn_{12}$ by 33.8 kcal mol^{-1} and uncapped γ-$NaSn_{12}$ by 23.8 kcal mol^{-1}. The cap on γ-$NaSn_{13}$ yields a short Sn-Sn distance of 3.15 Å. between the cap and the nearest tin, which might destabilize the single-capped γ-$NaSn_{13}$ by repulsion, compared to the uncapped γ-$NaSn_{12}$.[9] However, the uncapped γ-$NaSn_{12}$ is not observed. One analysis of these values is that a ΔG_{aq} of 23.8 kcal mol^{-1} between a capped and uncapped system is in fact sufficient to prevent the respective uncapped system from forming.

Synthesis strategy IV performed by Zhu *et al.* in 2019 produced double-capped γ-$NaSn_{14}$.[10] Authors were able to use borate ligands to stabilize the two capping butyltin, which in turn prevented isomerization in solution.[10] It is possible that a more symmetric structure with two caps rather than one allows for a more thermodynamically stable state. The computational results performed in this study indicate that double-capped γ-$NaSn_{14}$ is more stable than uncapped β-$NaSn_{12}$ by 55.1 kcal mol^{-1} and uncapped γ-$NaSn_{12}$ by 65.1 kcal mol^{-1}, as is shown in Figure 3. It seems that since this double-capped γ-$NaSn_{14}$ is more stable than its uncapped counterpart, it dominates in solution. Also, it is possible that since double-capped γ-$NaSn_{14}$ is 55.1 kcal mol-1 more stable than β-$NaSn_{12}$, it prevents uncapped-β from forming.

More structures in the Keggin cluster chemical space of Na-Sn need to be synthesized and computationally modeled to truly determine the influence of capping on the thermodynamic stability landscape. What is the energy difference that defines the transition point between forming a mixture of uncapped and capped Keggin clusters, and forming a pure phase? For example, in synthesis strategy III, could uncapped β-$NaSn_{12}$ have been prevented from forming if single-capped γ-$NaSn_{13}$ had only been 23.8 kcal mol^{-1} less stable? Computational tools can be employed to tune the structure of single-capped γ-$NaSn_{13}$ slightly to see if there is room for improvement. If a variation of the single-capped γ-$NaSn_{13}$ is determined, new syntheses can be designed to create this system. This would remove the need to double-cap the structure, and thus maintain simplicity of the structure and a promising photoresist material for EUV lithography. It should be noted that these energy differences are specific to the level of theory, including the implicit solvation, employed in the computational investigation.

5. Conclusions

The understanding of the fundamental lithographic mechanisms at play during exposure of a Na-Sn Keggin photoresist, can be improved first by exploring the tunability of this Na-Sn Keggin system. Computational results provided vital insight towards understanding the nature of this unique system that favors the lower symmetry Keggin isomers, β and γ. The successful collaborative accumulation of computational and experimental results confirmed that the Sn-Keggin clusters represent the only Keggin ion family to this date that favors these lower symmetry isomers. To prevent a mixture of isomers, strategic capping proved to be successful when the hydrolysis Gibbs free energy differences were large enough. Future work will focus on further probing this Sn-Keggin system's possible capping combinations and changing the central heteroatom.

6. Acknowledgements

The authors gratefully acknowledge the support of the National Science Foundation, Center for Chemical Innovation, grant CHE-1606982.

7. References

[1] "Euv Lithography Finally Ready For Chip Manufacturing - IEEE Spectrum.", <https://spectrum.ieee.org/semiconductors/nanotechnology/euv-lithography-finally-ready-for-chipmanufacturing> (10 September 2019).

[2] Frederick, R. T., Diulus, J. T., Hutchison, D. C., Olsen, M. R., Lyubinetsky, I., Nyman, M., and Herman, G. S., "Surface characterization of tin-based inorganic EUV resists," Advances in Patterning Materials and Processes XXXV, C. K. Hohle and R. Gronheid, Eds., 6, SPIE (2018).

[3] Passarelli, J., Murphy, M., Del Re, R., Sortland, M., Dousharm, L., Vockenhuber, M., Ekinci, Y., Neisser, M., Freedman, D. A., *et al.*, "High-sensitivity molecular organometallic resist for EUV (MORE)," **Advances in Patterning Materials and Processes XXXII 9425**, T. I. Wallow and C. K. Hohle, Eds., 94250T, SPIE (2015).

[4] Cardineau, B., Del Re, R., Al-Mashat, H., Marnell, M., Vockenhuber, M., Ekinci, Y., Sarma, C., Neisser, M., Freedman, D. A., *et al.*, "EUV resists based on tin-oxo clusters," **Advances in Patterning Materials and Processes XXXI 9051**, T. I. Wallow and C. K. Hohle, Eds., 90511B, SPIE (2014).

[5] Saha, S., Park, D.-H., Hutchison, D. C., Olsen, M. R., Zakharov, L. N., Marsh, D., Goberna-Ferrón, S., Frederick, R. T., Diulus, J. T., *et al.*, "Alkyltin keggin clusters templated by sodium.," *Angew. Chem. Int. Ed. Engl. 56*(34), 10140–10144 (2017).

[6] Li, M., Manichev, V., Garfunkel, E. L., Gustafsson, T., Nyman, M., Hutchison, D., Feldman, L. C., and Yu, F., "Novel Sn-based photoresist for high aspect ratio patterning," **Advances in Patterning Materials and Processes XXXV**, C. K. Hohle and R. Gronheid, Eds., 19, SPIE (2018).

[7] Closser, K. D., Ogletree, D. F., Naulleau, P., and Prendergast, D., "The importance of inner-shell electronic structure for enhancing the EUV absorption of photoresist materials.," *J. Chem. Phys. 146*(16), 164106 (2017).

[8] Sharps, M. C., Frederick, R. T., Javitz, M. L., Herman, G. S., Johnson, D. W., and Hutchison, J. E., "Organotin Carboxylate Reagents for Nanopatterning: Chemical Transformations during Direct-Write Electron Beam Processes," *Chem. Mater.* (2019).

[9] Hutchison, D. C., Stern, R. D., Olsen, M. R., Zakharov, L. N., Persson, K. A., and Nyman, M., "Alkyltin clusters: the less symmetric Keggin isomers.," *Dalton Trans. 47*(29), 9804–9813 (2018).

[10] Zhu, Y., Olsen, M. R., Nyman, M., Zhang, L., and Zhang, J., "Stabilizing γ-Alkyltin-Oxo Keggin Ions by Borate Functionalization.," *Inorg. Chem. 58*(7), 4534–4539 (2019).

[11] Keggin, J. F., "Structure of the Molecule of 12-Phosphotungstic Acid," *Nature 131*(3321), 908–909 (1933).

[12] Zhang, F.-Q., Guan, W., Zhang, Y.-T., Xu, M.-T., Li, J., and Su, Z.-M., "On the origin of the inverted stability order of the reverse-Keggin $[(MnO_4)(CH_3)_{12}Sb_{12}O_{24}]^{6-}$: a DFT study of alpha, beta, gamma, delta, and epsilon isomers.," *Inorg. Chem. 49*(12), 5472–5481 (2010).

[13] Wills, L. A., Qu, X., Chang, I.-Y., Mustard, T. J. L., Keszler, D. A., Persson, K. A., and Cheong, P. H.-Y., "Group additivity-Pourbaix diagrams advocate thermodynamically stable nanoscale clusters in aqueous environments.," *Nat. Commun. 8*, 15852 (2017).

[14] Casasnovas, R., Ortega-Castro, J., Frau, J., Donoso, J., and Muñoz, F., "Theoretical p K_a calculations with continuum model solvents, alternative protocols to thermodynamic cycles," *Int. J. Quantum Chem. 114*(20), 1350–1363 (2014).

[15] Sundstrom, E. J., Yang, X., Thoi, V. S., Karunadasa, H. I., Chang, C. J., Long, J. R., and Head-Gordon, M., "Computational and experimental study of the mechanism of hydrogen generation from water by a molecular molybdenum-oxo electrocatalyst.," *J. Am. Chem. Soc. 134*(11), 5233–5242 (2012).

[16] Zhang, L., Dembowski, M., Arteaga, A., Hickam, S., Martin, N. P., Zakharov, L. N., Nyman, M., and Burns, P. C., "Energetic trends in monomer building blocks for uranyl peroxide clusters.," *Inorg. Chem. 58*(1), 439–445 (2019).

[17] Becke, A. D., "Density-functional thermochemistry. III. The role of exact exchange," *J. Chem. Phys. 98*(7), 5648 (1993).

[18] Hariharan, P. C. and Pople, J. A., "The influence of polarization functions on molecular orbital hydrogenation energies," *Theor. Chim. Acta 28*(3), 213–222 (1973).

[19] Wadt, W. R. and Hay, P. J., "Ab initio effective core potentials for molecular calculations. Potentials for main group elements Na to Bi," *J. Chem. Phys. 82*(1), 284–298 (1985).

[20] Marenich, A. V., Cramer, C. J., and Truhlar, D. G., "Universal solvation model based on solute electron density and on a continuum model of the solvent defined by the bulk dielectric constant and atomic surface tensions.," *J. Phys. Chem. B 113*(18), 6378–6396 (2009).

[21] Krishnan, R., Binkley, J. S., Seeger, R., and Pople, J. A., "Self-consistent molecular orbital methods. XX. A basis set for correlated wave functions," *J. Chem. Phys. 72*(1), 650 (1980).

[22] López, X., Maestre, J. M., Bo, C., and Poblet, J.-M., "Electronic Properties of Polyoxometalates: A DFT Study of α/β -$[XM_{12}O_{40}]$n - Relative Stability (M = W, Mo and X a Main Group Element)," *J. Am. Chem. Soc. 123*(39), 9571–9576 (2001).

[23] Armstrong, C. R., Casey, W. H., and Navrotsky, A., "Energetics of Al_{13} Keggin cluster compounds.," **Proc. Natl. Acad. Sci. USA 108**(36), 14775–14779 (2011).

[24] Wang, W., Fullmer, L. B., Bandeira, N. A. G., Goberna-Ferrón, S., Zakharov, L. N., Bo, C., Keszler, D. A., and Nyman, M., "Crystallizing elusive chromium polycations," *Chem 1*(6), 887–901 (2016).

[25] Wang, W., Amiri, M., Kozma, K., Lu, J., Zakharov, L. N., and Nyman, M., "Reaction Pathway to the Only Open-Shell Transition-Metal Keggin Ion without Organic Ligation," *Eur J Inorg Chem 2018*(42), 4638–4642 (2018).

[26] López, X. and Poblet, J. M., "DFT study on the five isomers of PW(12)O(40)(3)(-): relative stabilization upon reduction.," *Inorg. Chem. 43*(22), 6863–6865 (2004).

[27] López, X., Carb., J. J., Bo, C., and Poblet, J. M., "Structure, properties and reactivity of polyoxometalates: a theoretical perspective.," *Chem. Soc. Rev. 41*(22), 7537–7571 (2012).

BACUS N • E • W • S

Industry Briefs

Semiconductor Makers' Pricing is Based not just on Quantities Ordered but also on "Capacity Rationing"

By **Tom Petruno,** UCLA Anderson School of Management, Semiconductor Packaging News

A standard assumption in business is that you get a discount for buying in quantity. But a study of business-to-business sales of IC's seems to turn that thinking on its head. In a surprising number of cases — about 26% of transactions studied over a three-year period — the manufacturer charged more per chip for large quantities than for smaller quantities of the same chip. One desktop computer chip sold for an average price of $29.13 to small-batch buyers, while large-batch customers paid a hefty 54% more, or $45.01 per chip.

Pricing decisions are based not just on the quantities ordered but also on "capacity rationing." The semiconductor market has short product life cycles and high capital investment requirements and is subject to intense initial price negotiations. A chip producer needs a certain number of large-quantity buyers to accelerate the selling process. Smaller-quantity buyers, meanwhile, are needed to consume "residual" manufacturing capacity. Then the producer needs to allow for mid-sized buyers to take up capacity that is too much for small buyers but not enough for large buyers.

The chip industry's selling regime differs from those of most other manufacturing sectors. Many companies naturally seek to achieve maximum sales, and price their goods accordingly, rewarding bigger-volume buyers with discounts if feasible. But in the case of semiconductors, manufacturing facilities are costly and construction lead times are long, while capacities are inflexible during a selling season.

There are some industries that do the same, such as the travel industry, where airline companies and hotels have limited capacities and these capacities have to be sold within a limited period. Customers in these industries include bulk buyers such as travel agencies and resellers who purchase different quantities and negotiated prices. Other examples may include movie theaters, concerts and sports events.

Monitoring for Excursions in Automotive Fabs

By **David W. Price, Jay Rathert, and Douglas G. Sutherland,** Kla Corp., Milpitas, CA

Semiconductor fabs that make automotive ICs offer service packages to ensure that the chips meet the stringent reliability requirements. But excursions are inevitable, as they are with any controlled process. Recognizing this, automotive semiconductor fabs create a comprehensive control plan to detect all excursions and keep "maverick" wafers from escaping the fab due to undersampling. It will clearly indicate which wafers are affected by each excursion so that they can be quarantined and more fully dispositioned – thereby ensuring that non-conforming devices will not inadvertently ship.

The control plan of an automotive service package will require much more extensive inspection and metrology than the control plan for production of ICs for consumer products. The fabs use approximately 1.5 to 2 times more defect inspection steps with more frequent sampling for automotive flows with additional sensitivity to capture the smaller defects that may affect reliability. The combined impact of these factors results in the typical automotive fab requiring 50% more process control capacity than their consumer product peers. As a result, if there is a defect excursion, it will be found much more quickly in the automotive flow. This limits the lots at risk: a smaller and more clearly defined population of lots are exposed to the higher defect count, thereby helping serve the traceability requirement. The excursion lots are then quarantined for high-sensitivity inspection of 100% of the wafers to disposition them for release, scrap, or a downgrade to a non-automotive application.

The additional inspection points in the automotive service package have the added benefit of simplifying the search for the root cause of the excursion by reducing the range of potential sources. Fewer potential sources help speed effective investigations to find and fix the problem. Counterintuitively, the increased number of inspection points also tends to reduce production cycle time due to reduced variability in the line.

One risk is that, because each wafer may take a unique path through the multitude of processing chambers in the fab, the sum of minor variations and marginalities across hundreds of process steps can create "maverick" wafers. These wafers can easily slip through a control plan that relies heavily on sub-sampling, allowing at-risk die into the supply chain. To address this issue, many automotive fabs are adding high-speed macro defect inspection tools to their fleet to scan more wafers per lot. This significantly improves the probability of catching maverick wafers preventing them from entering the automotive supply chain.

www.semiconductordigest.com

Join the premier professional organization for mask makers and mask users!

About the BACUS Group

Founded in 1980 by a group of chrome blank users wanting a single voice to interact with suppliers, BACUS has grown to become the largest and most widely known forum for the exchange of technical information of interest to photomask and reticle makers. BACUS joined SPIE in January of 1991 to expand the exchange of information with mask makers around the world.

The group sponsors an informative monthly meeting and newsletter, BACUS News. The BACUS annual Photomask Technology Symposium covers photomask technology, photomask processes, lithography, materials and resists, phase shift masks, inspection and repair, metrology, and quality and manufacturing management.

Individual Membership Benefits include:

- Subscription to BACUS News (monthly)
- Eligibility to hold office on BACUS Steering Committee

spie.org/bacushome

Corporate Membership Benefits include:

- 3-10 Voting Members in the SPIE General Membership, depending on tier level
- Subscription to BACUS News (monthly)
- One online SPIE Journal Subscription
- Listed as a Corporate Member in the BACUS Monthly Newsletter

spie.org/bacushome

CALENDAR

2020

Photomask Japan
19-20 April 2020
Yokohama, Japan

The 36th European Mask and Lithography Conference, EMLC 2020
22-24 June 2020
Leuven, Belgium

SPIE Photomask Technology + EUV Lithography
20-24 September 2020
Monterey Conference Center and Monterey Marriott
Monterey, California, USA

SPIE is the international society for optics and photonics, an educational not-for-profit organization founded in 1955 to advance light-based science and technology. The Society serves more than 255,000 constituents from 183 countries, offering conferences and their published proceedings, continuing education, books, journals, and the SPIE Digital Library in support of interdisciplinary information exchange, professional networking, and patent precedent. In 2019, SPIE provided more than $5 million in community support including scholarships and awards, outreach and advocacy programs, travel grants, public policy, and educational resources. **spie.org**

SPIE.
International Headquarters
P.O. Box 10, Bellingham, WA 98227-0010 USA
Tel: +1 360 676 3290
Fax: +1 360 647 1445
help@spie.org • **spie.org**

Shipping Address
1000 20th St., Bellingham, WA 98225-6705 USA

Managed by SPIE Europe
2 Alexandra Gate, Ffordd Pengam, Cardiff,
CF24 2SA, UK
Tel: +44 29 2089 4747
Fax: +44 29 2089 4750
spieeurope@spieeurope.org • **spieeurope.org**

You are invited to submit events of interest for this calendar. Please send to lindad@spie.org.